SciVerse ScienceDirect

Physics Procedia 22 (2011) 8 – 13

Physics Procedia

2011International Conference on Physics Science and Technology

Transport Properties of Single Vanadium Oxide Nanowire

Kien Wen Sun*

Department of Applied Chemistry, National Chiao Tung University, Hsinchu 30010

Abstract

We measured I-V characteristics and electrical resistance, in the temperature range from room temperature to above 600 K in order to obtain nanodevices. Measurements were taken on a single V_2O_5 nanowire deposited on a Si template, where two-point and four-point metallic contacts were previously made using e-beam lithography. In both two- and four-point probe measurements, the I-V curves were clearly linear and symmetrical with respect to both axes. Drastic reduction in electrical resistance and deviation from single valued activation energy with increasing temperature indicated phase transitions taking place in the nanowire. From temperature-dependent HR-Micro Raman measurements, reductions from V_2O_5 to VO_2/V_2O_3 phases took place at a temperature as low as 500 K, when electrons were injected to the nanowire through electrical contacts.

PACS: 73.21.Hb; 73.63.-b; 73.63.Nm

keywords: dielectrophoresis; metal oxide; phase transition; nanowire

1. Introduction

Recently, there has been a great interest on new types of nanodevices based on metal-oxide nanowires or nanotubes. Metal oxides with one-dimensional (1D) structures, such as a nanowire, nanotube, nanorods, and nanoribbon, show unique physical and chemical properties because of their large surface area and unique shape, making these materials effective for applications in photovoltaic devices [1-3], field emission display [4,5], and so on. Therefore, synthesizing novel metal-oxide nanostructures and probing their intrinsic properties are critical to assess their possible role in new types of nanoscale devices.

Among these metal oxide semiconductors, vanadium pentoxide has attracted considerable interest over the years owing to its wide range of applications. Vanadium oxide and its derivated compounds [6] have been applied in catalytic and electrochemical fields due to their outstanding structural flexibility combined with chemical and physical properties [7,8]. Vanadium pentoxide oxide phase crystallized in 2D network structures can be regarded as a layered structure compound in which VO_5 square pyramids with a five-fold coordination of vanadium and oxygen

* Corresponding author. Tel.: +0-000-000-0000 ; fax: +0-000-000-0000 .
E-mail address: kwsun@mail.nctu.edu.tw

1875-3892 © 2011 Published by Elsevier B.V. Selection and/or peer-review under responsibility of Garry Lee.
doi:10.1016/j.phpro.2011.11.004

atoms are connected by sharing corners and edges [9]. V_2O_5 has a bandgap of ~ 2.5 eV. Prospective applications include photo- and electro-chromic devices [1,3], chemical and gas sensing [10-13], catalysis [14], and positive electrodes of rechargeable lithium battery [15,16].

V_2O_5 with a 1D nanostructure has been successfully synthesized via template-assisted growth [17], surfactant/inorganic self-assembly, e-beam sputtering, chemical vapor deposition [18], pulse laser deposition [19,20], hydrothermal approach [17,21-23], and vapor pyrolytic deposition [24]. The electrical transport mechanism in V_2O_5 nanofibers has been studied in detail [25,26] at low temperature and room temperature. The conductivity of an individual V_2O_5 fiber was estimated to be ~ 0.5 S/cm at 300 K. N-type enhancement FET-like behavior was demonstrated for individual V_2O_5 nanofibers at low temperature. The charge transport takes place through electron hopping between V^{IV} (impurities) and V^{V} centers. Chemiresistor-type gas sensors with high sensitivity and selectivity to amines were fabricated by depositing V_2O_5 nanofibers onto silicon templates [27]. More recently, I-V characteristics and electrical resistance were measured on V_2O_{5-x} – polyaniline nanorods with inter-digital metallic contacts made by lithography [28] from 300 - 140 K. The I-V curves were nonlinear and symmetrical with electrical conductivity values near 0.1 S/cm at room temperature. In this present work, resistivity of a single V_2O_5 nanowire and contact resistance were accurately determined using three different probe schemes at room temperature. The wire was also transformed from a phase of pure V_2O_5 into mixed phases containing V_2O_3 and VO_2 at a temperature as low as 500 K when under electrical bias.

2. Experimental

Our V_2O_5 nanowires were grown on a conducting glass substrate combining gaseous transport and pyrolytic deposition of vanadium polyoxometalate anions, which yield vertically aligned V_2O_5 nanowires. The XRD pattern of the nanowires was indexed to the orthorhombic V_2O_5 structures. No signals due to impurity phases were detected. The HR-TEM image and SAED pattern confirm that the grown nanowires are single crystalline in nature and grown preferentially along one direction [010]. The synthesized V_2O_5 wires show ribbon-like morphology with an average width within 200 - 500 nm and a length up to several tens of micrometers. Details of the crystal growth and characterizations have been published elsewhere [24].

Fabrication processes of the single nanowire-based devices are given as follows. The V_2O_5 nanowire powder was first diluted in 10 ml deionized (DI) water and ethanol (or acetone) mixture. The solution was then placed in an ultrasonic bath operated at a vibration frequency of 185 KHz for 30 min to prevent cluster formation. A test drop of the solution was placed on a bare Si wafer. After the solution dried out, scanning electron microscope (SEM) images were taken to examine nanowire clustering. The concentration of the solution was continuously diluted and adjusted until the nanostructures can be well dispersed on the Si template.

Two-point and four-point metal contacts on Si templates were designed and fabricated to position a dispersed single nanowire. The templates used were commercially available 4-inch silicon wafers with (001) crystal orientation and n-type background doping. The surface of the Si substrate was passivated in advance using a thermally grown SiO_2 layer with a thickness of 2000 Å. This was to avoid leakage current through the substrate during current–voltage (I-V) measurements. The Si wafer was first diced into 2 x 2 cm chips. A pattern of two-dimensional arrays of cross-finger-type Al or Ti/Au pads with a line width of ~ 2 μm, a pitch from 2 - 10 μm, and a length of ~ 15 μm were defined on the Si chip using e-beam lithography within an area of 1 mm^2.

A drop of the properly diluted V_2O_5 nanowire solution was placed within the inter-digitated electrode patterns. By applying electrical bias across the contact pads, the dielectrophoresis force [29-32] drove the nanowires to bridge the electrode gap. The SEM images of the V_2O_5 nanowires' dielectrophoresis alignment process across the inter-digitated electrodes are shown in Figure 1. The sample surface was scanned by SEM to allocate a single nanowire across two or four metal contacts. After a single nanowire was selected, a focus ion beam (FIB) was used to selectively deposit Platinum (Pt) metal contacts on the wires, as shown in Figure 2. The patterned single nanowire was examined with EDX to ensure it was not contaminated during the FIB process. Temperature dependence of the I-V characteristics of a single V_2O_5 nanowire was probed at a temperature range from 300 - 640 K. This was done with an HP-4145 probe station under current sensitivity of 1 pA and heating stage. The resistivity of the single nanowire at 300 K was determined with three different probe schemes: (a) Two-point contact probe (sweep voltage mode), where current through the wire was measured by sweeping the voltage from -0.5 - 0.5 V with a step of 0.001 V; (b) Four-point contact probe (sweep current mode), where current was supplied through outer electrodes and voltage drop was determined between two inner electrodes; and (c) Four-point contact probe, where resistivity of the nanowire was determined using an algorithm developed by Gu et al. [33]. The Raman spectra of the single wire

under the temperature-dependent electrical measurements were monitored at the same time through a confocal microscope. The spectra were then analyzed by a 0.8 m spectrometer equipped with liquid nitrogen cooled CCD detector at the excitation wavelength of 633 nm.

Figure 3 shows the I-V curve of a nanowire dispersed in ethanol and prepared on two-point Al electrodes. At room temperature, the sample exhibited slightly nonlinear, symmetrical I-V characteristics. The Schottky type contact resistance between the nanowire and Al contact was due to the nanowire adsorption of ethanol molecules [34]. The contact problem was solved when nanowires were dispersed in solutions containing no hydrogen bonds, such as acetone. Figure 4 shows the improved I-V characteristics of the single wire dispersed in acetone and prepared on two-point Au electrodes. Contact between the wire and the electrodes now show linear and symmetrical behavior. A resistivity of 6.61 Ω–cm of the device was derived from various samples. Contact resistance can be determined by comparing results between two- and four-point probe measurements. The single wire resistivity determined with probe scheme (b) is 5.87 Ω–cm, resulting in a contact resistance ~ 50.305 KΩ. The resistivity value was further verified using probe scheme (c). The schematic of probe scheme (c) and the parameters used to derive the resistivity are summarized in Table I. The derived resistivity is 5.65 Ω–cm, which is very close to the result determined from probe scheme (b).

Following the electrical characterization of the single wire at room temperature, individual nanowires were placed on a heating stage in a chamber. Measurements of temperature dependence in conductivity were first carried out at atmosphere in the temperature range 300 – 580 K. The resistance of the single nanowire is plotted in Figure 5 as ln(T/R) versus reciprocal temperature. Electrical conduction in V_2O_5 is generally believed to proceed by hopping between V^{5+} and V^{4+} impurity centers [25,35]. An increase in conductivity with increasing temperature was revealed, consistent with thermally activated hopping transport. However, the curve departed significantly from linearity when the plot of ln(T/R) versus 1/T in Figure 5 was analyzed using a model proposed by Mott [36] for small polaron hopping in transition metal oxides. A similar behavior was also observed in electrical measurements at lower temperature [25]. This has been attributed to the temperature dependence of the hopping activation energy, which includes a disorder energy associated to the random material structure [37]. The departure from linearity was even more pronounced when the temperature was further increased. We also noted that the conductivity of the nanowire was not completely restored to its original value after it cooled down to room temperature. On the other hand, the nanowire was relatively stable if simply heated it up to 600 K without applying electrical bias. Therefore, a phase transformation is suspected to be taking place during heating processes, and the phase transitions are facilitated by the injection of electrons through the contacts.

In the next experiments, the sample chamber was pumped down and flushed with dry N_2 three times. Then the temperature-dependent measurements in conductivity were carried out both in vacuum and at an inert gas (N_2) filled environment at the temperature range of 300 – 550 K. Figure 6 shows the resistance of the single nanowire plotted as ln(T/R) versus reciprocal temperature. The resistance of the nanowire dropped by three orders of magnitude from 1.7 MΩ at 300 K to 1.725 KΩ at 550 K. The latter value was maintained without breaking the vacuum after the wire cooled down to 300 K. The curve in Figure 6 strongly deviated from a linear plot. During the measurements, evolutions of the Raman spectra as a function of temperature were also monitored simultaneously at each temperature increment step. The Raman spectrum of the V_2O_5 nanowire recorded before the temperature-dependent electrical measurements is shown in Figure 7 (a). The Raman lines at 143, 283, 404, 482, 525, 699, and 994 cm^{-1} are assigned to V_2O_5 in its orthorhombic phase [38,39]. As the temperature was increased to above 500 K, changes were observed in the spectra and new lines began to appear. The Raman spectrum of the sample at the end of the temperature cycle is given in Figure 7 (b). The assignment of the peaks is summarized in Table II. After comparing our results with Raman spectra from pure V_2O_3 and VO_2, we conclude that the reduction in resistance of nanowire is most likely due to the appearance of the V_2O_3 and VO_2 phases. Self-assembled VO_2 nanowires have been synthesized by pyrolysis of $(NH_4)_{0.5}V_2O_5$ nanowires in vacuum at a temperature as high as 800 - 870 K [40]. However, transitions into V_2O_3 and VO_2 phases can take place at a temperature as low as 500 K when the V_2O_5 nanowire is under electrical bias, i.e., electrons are supplied through the contact to the nanowire. The change in resistance was clearly more drastic when temperature-dependent measurements were carried out in the inert gas filled environment and in vacuum. This is because that transitions to V_2O_3 and VO_2 phases are hampered by the re-oxidation process when the nanowire is exposed to the O_2. This is also the reason why the resistance of the nanowire maintains at its final value in inert gas filled and vacuum environment.

3. Conclusion

In conclusion, the transport properties and temperature dependence in conductivity of single V_2O_5 nanowires using e-beam lithography, FIB, and dielectrophoresis techniques were reported. I-V characteristics showed linear and symmetric behavior through the entire temperature range, which indicated that the contacts are ohmic. The resistivity and contact resistance were accurately determined using three different probe schemes. Resistance of the single V_2O_5 nanowire decreased with increasing temperature due to the occurrence of mixed V_2O_3/VO_2 phases. The temperature dependence of the nanowire transport characteristics shows a drastic reduction in electrical resistivity (by three orders of magnitude) at a temperature near 550 K. Evidence from the Raman spectra indicate that phase transitions take place at a temperature as low as 500 K when the nanowire is under an electrical bias.

Acknowledgment

This work was supported by a grant from the National Science Council, ROC (NSC 99-2119-M-009-004-MY3).

References

[1] Cheng, K.-C.; Cheng, F.-R.; Kai, J.-J. *Sol. Energy Mater. Sol. Cell* 2006, 90, 1156.
[2] Law, M.; Greene, L.E.; Johnson, J.C.; Saykall, R.; Yang, P.D. *Nature* 2005, 4, 455.
[3] Nishio, S. *Chem. Mater.* 2002, 14, 3730.
[4] Chen, W.; Zhou, C; Mai, L.; Liu, Y.; Qi, Y.; Dai, Y. *J. Phys. Chem. C* 2008, 112, 2262.
[5] Zhou, C.; Mai, L.; Liu, Y.; Qi, Y.; Dai, Y.; Chen, W. *J. Phys. Chem. C* 2007, 111, 8202.
[6] Zavalij, P.Y.; Whittingham, M.S. *Acta Crystallogr.* 1999, 855, 627.
[7] Spahr, M.E.; Stoschitzkj-Bitterli, P.; Nesper, R.; Haas, O.; Novak, P. *J. Electrochem. Soc.* 1999, 146, 2780.
[8] Braithwaite, J.S.; Catlow, C.R.A.; Gale, J.D.; Harding, J.H. *Chem. Mater.* 1999, 11, 1990.
[9] Bachmann, H.G.; Ahmed, F.R.; Bames, W.H. *Z. Kristallogr.* 1961, 15, 110.
[10] Oyama, S.T.; Went, G.T.; Lewis, K.B.; Bell, A.T.; Somorjait, G.A. *J. Phys. Chem. B* 1999, 93, 6786.
[11] Mao, C.-J.; Pan, H.-C.; Wu, X.-C.; Zhu, J.-J.; Chen, H.-Y. *J. Phys. Chem. B* 2006, 110, 14709.
[12] Dhayal Raj, A.; Pazhanivel, T.; Suresh Kumar, P.; Mangalaraj, D.; Nataraj, D.; Ponpandian, N. *Current Appl. Phys.* 2010, 10, 531.
[13] Raible, I.; Burghard, M.; Schlecht, U.; Yasuda, A.; Vossmeyer, T. *Sensors and Actuators B* 2005*,* 106, 730.
[14] Chen, L.; Yang, B.; Zhang, X.; Dong, W.; Cao, K.; Zhang, X. *Energy Fuels* 2006, 20, 915.
[15] Chan, C.K.; Peng, H.; Twesten, R.D.; Jarausch, K.; Zhang, X.F.; Cui, Y. *Nano Lett.* 2007, 7, 490.
[16] Protasenko, V.; Gordeyev, S.; Kuno, M. *J. Am. Chem. Soc.* 2007, 129, 13160.
[17] Shi, S.; Cao, M.; He, X.; Xie, H. *Cryst. Growth Des.* 2007, 7, 1893.
[18] Díaz-Guerra, C.; Piqueras, J. *Cryst. Growth Des.* 2008, 8, 1031.
[19] Barreca, D.; Armelao, L.; Caccavale, F.; Noto, V.D.; Gregori, A.; Rizzi, G.A.; Tondello, E. *Chem. Mater.* 2000, 12, 98.
[20] Ramana, C.V.; Smith, R.J.; Hussain, O.M.; Chusuei, C.C.; Julien, C.M. *Chem. Mater.* 2005, 17, 1213.
[21] Zhou, F.; Zhao, X.; Yuan, C.G.; Li, L. *Cryst. Growth Des.* 2008, 8, 723.
[22] Chen, W.; Zhou, C.; Mai, L.; Liu, Y.; Qi, Y.; Dai, Y. *J. Phys. Chem.* C 2008, 112, 2262.
[23] Mai, L.; Guo, W.; Hu, B.; Jin, W.; Chen, W. *J. Phys. Chem. C* 2008, 112, 423.
[24] Wu, M.-C.; Lee, C.-S. *J. Solid State Chem.* 2009, 182, 2285.
[25] Muster, J.; Kim, G.T.; Krstic, V.; Park, J.G.; Park, Y.W.; Roth, S.; Burghard, M. *Adv. Mater.* 2000, 12, 420.
[26] Kim, G.T.; Muster, J.; Krstic, V.; Park, J.G.; Park, Y.W.; Roth, S.; Burghard, M. *Appl. Phys. Lett.* 2000, 76, 1875.
[27] Raible, I.; Burghard, M.; Schlecht, U.; Yasuda, A.; Vossmeyer, T. *Sensor and Actuators B* 2005, 106, 730.
[28] Ferrer-Anglada, N.; Gorri, J.A.; Muster, J.; Liu, K.; Burghard, M.; Roth, S. *Mater. Sci. & Engineering C* 2001*,* 15, 237.
[29] Yamamoto, K.; Akita, S.; Nakayama, Y. *Jpn. J. Appl. Phys.*, 1996, 35, L917-L918.
[30] Yamamoto, K.; Akita, S.; Nakayama, Y. *J. Phys. D: Appl. Phys.* 1998, 31, L34-L36.
[31] Choi, W.B.; Jin, Y.W.; Kim, H.Y.; Lee, S.J.; Yun, M.J.; Kang, J.H.; Choi, Y.S.; Park, N.S.; Lee, N.S.; Kim, J.M. *Appl. Phys. Lett.* 2001, 78, 1547-1549.
[32] Suehiro, J.; Zhou, G.; Hara, M. *J. Phys. D: Appl. Phys.* 2003, 36, L109-L114.
[33] Gu, W.; Choi, H.; Kima, K. *Appl. Phys. Lett.* 2006, 89, 253102.

[34] Liu, J.; Wang, X.; Peng, Q.; Li, Y. *Adv. Mater.* 2005, 17, 764-767.
[35] Livage, J. *Chem. Mater.* 1991, 3, 578.
[36] Mott, N.F. *J. Non-Cryst. Solids* 1968, 1, 1.
[37] Bullot, J.; Gallais, O.; Gauthier, M.; Livage, J. *Appl. Phys. Lett.* 1980, 36, 986.
[38] Oyama, S.T.; Went, G.T.; Lewis, K.B.; Bell, A.T.; Somorjait, G.A. *J. Phys. Chem. B* 1999, 93, 6786.
[39] Wang, J.; Gonsalves, K.E. *J. Comb. Chem*. 1999, 1, 216.
[40] Wu, X.; Tao, Y.; Dong, L.; Wang, Z.; Hu, Z. *Mater. Res. Bull.* 2005, 40, 315-321.

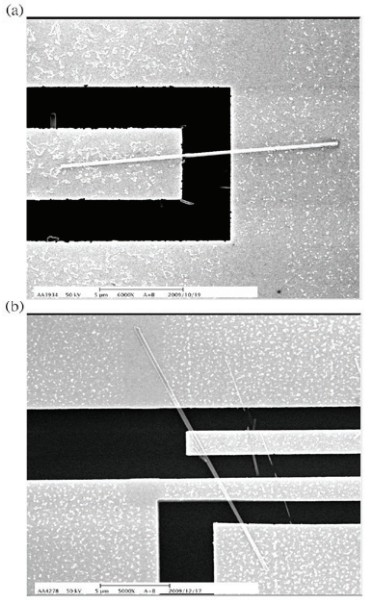

Figure 1(a) and (b) Nanowires aligned across the gaps between electrodes due to the dielectrophoresis force. on the

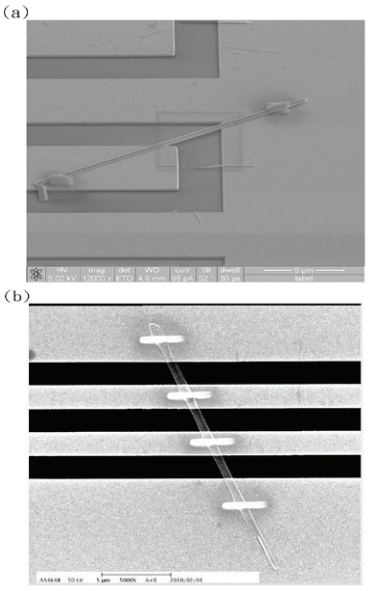

Figure 2(a) and (b) Contacts to electrodes were made by depositing Platinum (Pt) metal nanowires using focusing ion beam.

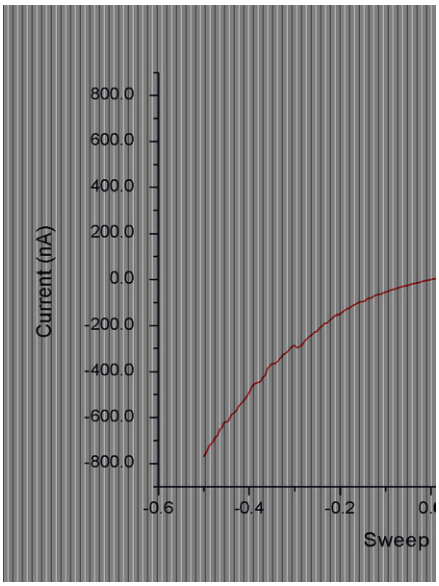

Figure 3 I-V characteristics of the single dispersed in ethanol at room temperature.

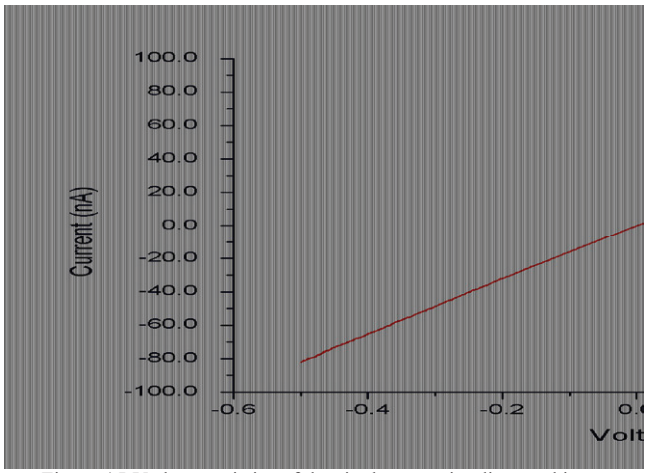

Figure 4 I-V characteristics of the single nanowire dispersed in aceton at room temperature.

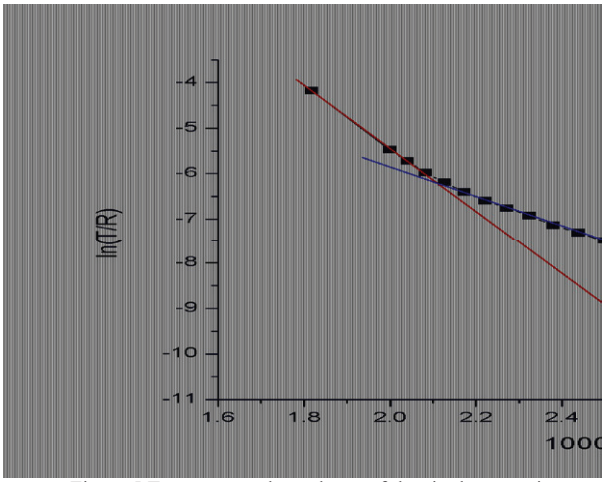

Figure 5 Temperature dependence of the single nanowire measured at atmosphere. The plot was approximated by a straight line (in red color) in the high temperature range (T > 500 K).

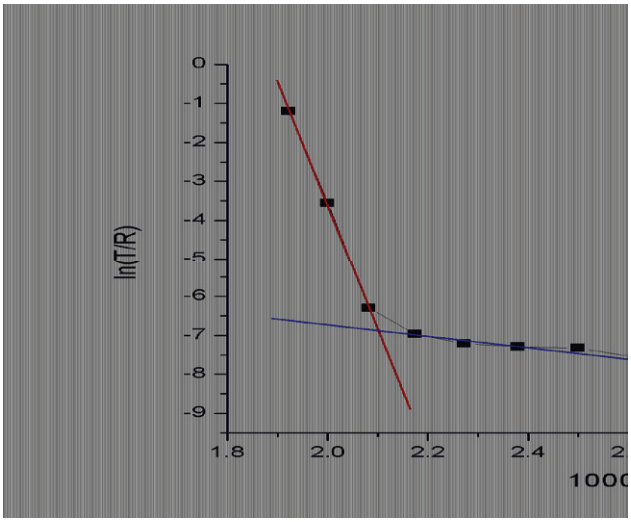

Figure 6 Temperature dependence of the single nanowire measured at atmosphere. The plot was approximated by a straight line (in red color) in the high temperature range (T > 500 K).

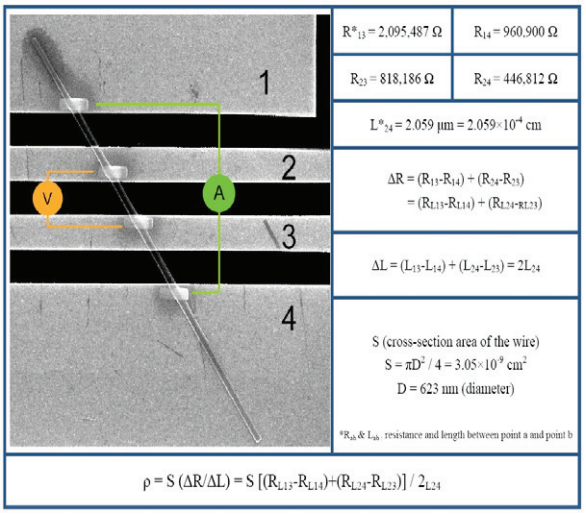

Table I. Schematic of the probe scheme (c) and parameters used to derive the resistivity of the single wire.

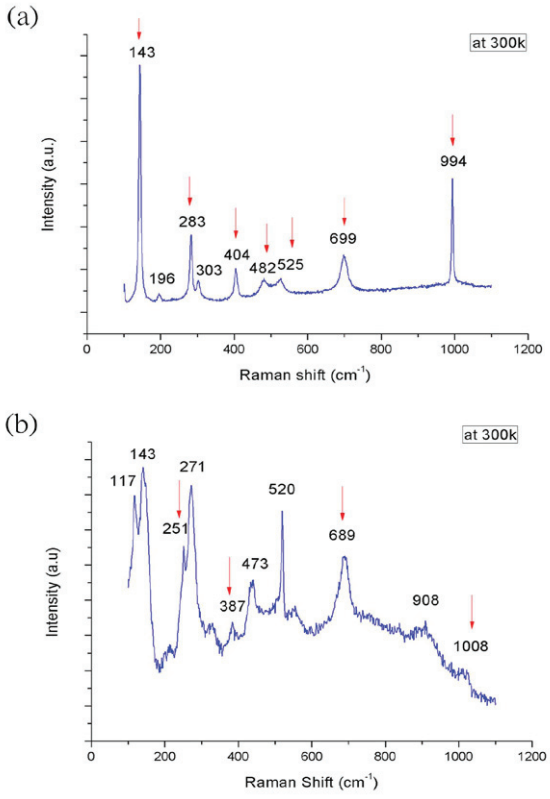

Figure 7 Raman spectrum of the single V_2O_5 nanowire under electrical bias (a) at the beginning of temperature cycle. (b) at the end of the temperature cycle. Peaks in (a) indicated by red arrows are signatures from the V_2O_5 phase. Peaks in (b) indicated by red arrows are signatures from the VO_2/V_2O_3 phase.

Raman peak (cm^{-1})	Assignment
117	Acetone
143	V_2O_5 (V-O-V sym-related stretch)
251	V_2O_3
271	Gold electrode (Au)
387	VO_2 (Ag mode)
437	Ethanol (C-C-O in-plane bend)
520	Si substrate (Si)
689	$V_2O_3^{4+}$ (V-O-V)
908	ACE (C-C stretch)
1008	$V_2O_3^{4+}$ (V=O)

Table II. List of peak assignment of the Raman spectrum shown in Figure 7 (b).